



## PERFORMANCE EVALUATION OF MICRO AUTOMATIC PRESSURE MEASUREMENT SENSOR FOR ENHANCED ACCURACY

SHUIQUAN ZHU\*

**Abstract.** The major objective of this research is to design sensitive components, conversion components, and various sensor circuits to achieve the miniaturization design for more accurate measurements. This article conducts performance testing on the designed miniaturized pressure sensor to determine whether it meets the qualified standards. The response time of designed sensor results increases with the increase of pressure under experimental conditions of different pressure application values (5MPa to 50MPa). The detection accuracy of the micro automatic pressure measurement sensor designed in this paper can reach 0.0452%; the average pressure is 0.00364%, and the insulation resistance is 68.44 megohms, which meets reliability requirements. The sensitivity is 0.0582%; the nonlinearity is 0.0741%; the hysteresis is 0.0266%; The repeatability of 0.0625% meets the qualification standard for this instrument. Still, compared with traditional sensors, the sensor reduces the response time of results by about 60%. However, the author conducted the detection in an ideal environment. The actual working environment of sensors is relatively good. Therefore, the detection results obtained in this article may have some errors compared to the actual situation, and further analysis and testing are needed to optimize the performance of the designed sensor.

**Key words:** Micro-mechanical electronic technology, automatic measurement sensor, sensitive diaphragm, conversion element

**1. Introduction.** Sensors are one of the most representative achievements in modern science and technology development and have the same status as communication technology and computer technology used for inertial navigation and space attitude determination [1]. Biosensors, fluid sensors, etc., are used in biomedicine for clinical measurements and pathological diagnosis [2]. In environmental monitoring, temperature, humidity, and gas sensors are used to monitor changes in the surrounding environment to determine whether pollution or adverse weather has occurred [3]. To meet the requirements of more refined monitoring work, sensors are gradually developing toward more intelligence, automation and miniaturization. Micro-detectors are micro-sensors, the most commonly used field in miniaturization development. Based on the different uses and types of microsensors, sensors are divided into capacitive MEMS differential pressure sensors, magnetic field measurement microsensors, Hall-type magnetic liquid micro differential pressure sensors, etc. [4,5]. Based on this, the author selects a commonly used automatic pressure measurement sensor as the object to research the design of automatic measurement sensors for micro-mechanical electronic technology. The design is divided into two parts: theoretical design and application testing. It includes several modules, such as sensitive diaphragm design, conversion element design, signal conversion circuit design, sensor interface circuit design and working program design [6,7].

Figure 1.1 shows a reference for producing and manufacturing microsensors and promotes the application and development of micromechanical electronic technology.

**2. Literature Review.** In recent years, issues such as medical diagnosis, environmental hygiene, and food safety have occurred frequently in China. This places higher demands on the rapid and real-time detection of viruses, antigens, and other substances, also known as point-of-care testing [8]. In 2014, the globally renowned market research company Persistence Market Research (PMR) released an authoritative survey report on the future development of biosensors. The report indicates that the global biosensor market will grow rapidly in the next six years. In 2014, the market value of biosensors was \$12.9 billion, and by 2020, the market value will increase to \$22.5 billion, with a compound annual growth rate of 9.7% [9,10]. Among them, biosensors have the most applications in the POCT field, and the demand is also the largest and has been increasing continuously [11]. Therefore, it is urgent to research point-of-care detection technology, which has great economic and

---

\*Tianjin Electronic Information College, Tianjin, 300350, China (Corresponding author's e-mail: [shuiquanzhu@126.com](mailto:shuiquanzhu@126.com))

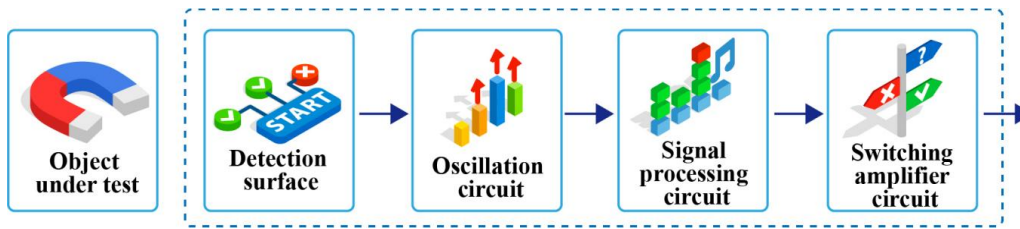


Fig. 1.1: Measurement process for automation control

social significance [12].

The basic principle of biosensors is that microelectronic control systems control the flow of sensitive membranes through the microfluidic environment of the tested object (antibodies, viruses, bacteria, etc.). The substance to be tested is adsorbed on the surface of the sensitive membrane, and the transducer converts the biological signals on the sensitive membrane into electrical signals. Then, it is measured through a dedicated signal detection system. Finally, the concentration and quality are achieved by measuring various characteristics of the sensors [13, 14]. In addition, driven by microelectromechanical systems (as well as microelectronics technology), piezoelectric biosensor systems are also developing towards automation, intelligence, and miniaturization. This lays a solid foundation for applying piezoelectric sensors in point-of-care testing (POCT) [15]. The researchers observed that an anisotropic crystal generates charges on the surface under external mechanical pressure. When the external force is removed, the surface charge disappears. This phenomenon is called the Piezoelectric effect [16]. The piezoelectric effect is divided into the positive and inverse piezoelectric effects. Specifically, the positive piezoelectric effect means that when an external force acts on the piezoelectric crystal in a certain direction, electric polarization will occur inside the crystal, at the same time, positive and negative charges are generated on the two surfaces of the crystal; When the crystal loses the external force, it is in an uncharged state; when an external force is applied in the other direction of the crystal, the charge polarity will be changed [17, 18]. Since the dielectric constant, elastic constant and piezoelectric constant of piezoelectric crystals tested with different boundary conditions have little difference in general, therefore, generally do not distinguish between the elastic constant of the circuit and the elastic constant of the short circuit, the free permittivity and the clamping permittivity, at this point, the relationship between the stress  $T$  and the electric field  $E$  in the piezoelectric crystal can be established, which is also the basis for this effect to be applied to automated measurement sensors [19].

### 3. Research Methods.

**3.1. Microsensors for MEMS.** The types of microsensors in the MEMS are different; the author uses the pressure sensor to conduct a design study. The pressure sensor is based on the piezoresistive effect combined with Ohm's law to estimate the pressure value. When a certain pressure is applied to the semiconductor material (sensitive diaphragm) from the outside, the material will undergo corresponding strain, and the strain will drive the resistance to change at the same time, at this time, the bridge will lose its balance and the corresponding voltage value will be output, then the actual pressure value can be converted by using Ohm's law [20, 21].

The mathematical Equation of resistance change is expressed as:

$$\frac{\Delta R}{R} \approx \pi_1 \sigma_1 + \pi_t \sigma_t \quad (3.1)$$

In Equation 3.1,  $\frac{\Delta R}{R}$  is the rate of change of the varistor;  $\pi_1$  and  $\pi_t$  represent the transverse piezoresistive coefficient and the longitudinal piezoresistive coefficient, respectively;  $\sigma_1$  and  $\sigma_t$  represent the transverse stress and the longitudinal stress, respectively.

When the semiconductor material (sensitive diaphragm) is not affected by the force, the four bridges are always in a balanced state, and the output voltage at this time = 0. Its Equation is expressed as

$$R_1 = R_2 = R_3 = R_4 = 0 \quad (3.2)$$

In Equation 3.2,  $R_1$ ,  $R_2$ ,  $R_3$ ,  $R_4$  and represent the resistance values of the four arms of the Wheatstone Bridge.

When the outside world pressures the semiconductor material (sensitive diaphragm), the bridge connected to it will be out of balance. At this time, the voltage output is expressed as

$$V_{out} = \frac{(R_1 + \Delta R)(R_3 + \Delta R) - (R_2 - \Delta R)(R_4 - \Delta R)}{(R_1 + R_2)(R_3 + R_4)} V_i \quad (3.3)$$

When  $R_1$ ,  $R_2$ ,  $R_3$ , and  $R_4$  are all equal to the same value, it can be simplified to formula 3.4:

$$V_{out} = \frac{\Delta R}{R} V_i \quad (3.4)$$

In the formula,  $V_i$  is the supply voltage.

Before designing, it is necessary to understand the structure and composition of the micro pressure sensor, that is, the design of the sensitive diaphragm, the design of the conversion element, the design of the signal conditioning and conversion circuit, the design of the sensor interface circuit, and the design of the sensor working program. These design modules are analyzed in detail [22].

**3.2. Sensitive Diaphragm Design.** The sensitive diaphragm is the most critical component in automatic measurement sensors, which can directly sense the measured value and is the only external force contactor and voltage output source. In this article, the sensitive diaphragm design adopts the MEMS etching process in silicon micromachining technology, and the specific process is as follows [23]:

Step 1: Select the substrate of the sensitive diaphragm, that is, the bearing part of the sensitive element. Here, single-crystal silicon is selected as the substrate of the sensitive diaphragm;

Step 2: Monocrystalline silicon processing. The production of the sensitive film needs to ensure that the single crystal silicon wafer is free of any damage, needs to be ground and polished, and then needs to be cleaned to remove impurities attached to the surface. After that, wait for etching;

Step 3: Etching active marks, that is, preparing alignment marks and scribing frames;

Step 4: Depositing a masking layer, that is, covering a layer of protective film on the monocrystalline silicon wafer;

Step 5: Open the varistor and the ohmic contact area, that is, remove part of the silicon on the back of the silicon wafer to form a cavity;

Step 6: The contact area is implanted with ions to form varistor strips;

Step 7: Standard cleaning monocrystalline silicon wafer;

Step 8: Deposition-layer  $SiO_2$ , as isolation layer;

Step 9: Use magnetron sputtering technology to sputter Ti-Pt-Au on the glass sheet to form an electrode plate;

Step 10: Photolithography of electrode hole area and lead area pattern;

Step 11: Reduce the thickness of the monocrystalline silicon wafer;

Step 12: Bonding the silicon wafer and glass together;

Step 13: Packaging.

To ensure the sensitivity and accuracy of the sensitive chip, the external environment should not be corrupted. It is necessary to use an isolation diaphragm to separate the sensitive diaphragm from the measured medium to avoid contamination and damage.

**3.3. Conversion Elements.** The automated measurement sensor in this study is a miniature pressure sensor, and its measurement principle is based on the piezoresistive effect; the crimp resistor is the transducer element of the sensor. The varistor is an electrical signal that converts the strain force of the sensitive abdominal piece feels into a resistance value. Then, it converts into a voltage in combination with the given supply voltage, so the varistor design is very important [24].

**3.4. Design of Signal Conditioning Circuit for Measurement Sensor.** The function of the signal conditioning conversion circuit is to amplify, modulate and filter the signal to improve the signal quality. Figure 3.1 is a signal conditioning conversion circuit designed for an automated measurement sensor.

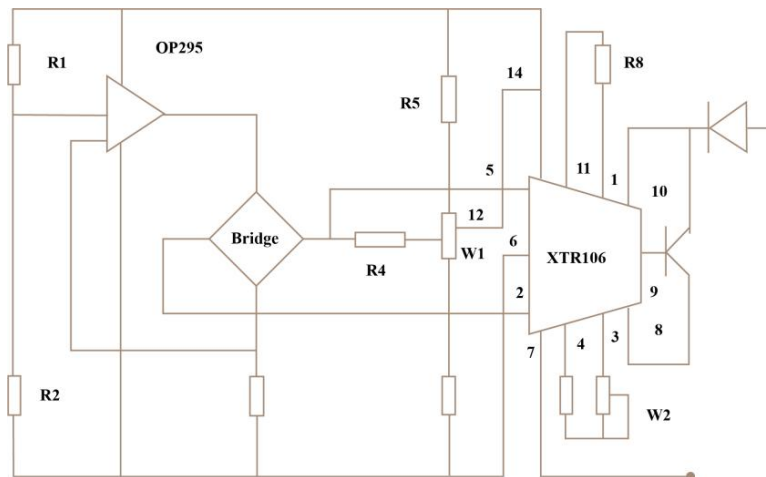


Fig. 3.1: Design of signal conditioning and conversion for the automatic measurement sensor

Table 3.1: The function table of each interface circuit pin of the sensor

Pin number	Pin symbol	Pin function
1	GND	Ground, Power negative
2	SYNC	Circuit common ground voltage
3	DVCC	Voltage into the circuit
4	VDD	The working voltage of the chip
5	NC	Empty feet for extended functions
6	V1P	Empty feet, please hang
7	V1N	The turn-off control signal of op-amp unit 1
8	V2N	Op-amp unit 2 shutdown control signal
9	V2P	Timer interrupt
10	RESET	The chip is not powered on, reset the sensor
11	AGND	Serial data, Single bus
12	GIN	Signal output
13	DGND	Digital analog
14	CLKOUT	Output a clock signal by default

**3.5. Sensor Interface.** The designed automatic measurement sensor is the main part of the micro-mechanical electronic system, so the sensor must be connected to other external devices. Therefore, the sensor interface design is reasonable, and the data collected by the sensor can be used directly by the MEMS system [25]. The sensor interface, also known as the pin, is the interface between the internal circuit and the peripheral device, and all the pins are the sensor's interface. There are 14 sensor pins, and each pin has different functions. Table 3.1 shows the pin functions of each interface circuit of the sensor.

**3.6. Sensor Working Procedure.** The automatic measurement sensor design belongs to the hardware category. In addition, it is necessary to write and design a working program to provide logical guidance. The working procedure of the sensor is the process of collecting data from the sensor. The steps of the sensor working procedure are as follows:

- Step 1: Initialize the sensitive chip;
- Step 2: Initialize each circuit;
- Step 3: Wait for the collection order;
- Step 4: Judge whether the acquisition command arrives. If it arrives, then enter the next step; otherwise,

Table 4.1: Dimensional Specifications for Microsensor Components in 3D and 2D Models

Geometry	3D model ( $\mu\text{m}$ )	2D model ( $\mu\text{m}$ )
Interdigital electrode width	5	5
Interdigital electrode length	40	-
Interdigital electrode thickness	0.3	0.3
Adjacent interdigital electrode spacing	5	5
Delay line width	40	500
Delay line length	40	-
Delay line thickness	0.3	0.3
Number of interdigitated electrode pairs	5+1 (pair)	20+20 (pair)
Waveguide layer width	200	910
Waveguide layer length	60	-
Waveguide layer thickness	2	2
Base width	200	910
Base length	60	-
Substrate thickness	40	300

enter the low power consumption state and return to the previous step;

Step 5: The sensor perceives the measured quantity;

Step 6: Utilize the conversion element to convert the measurement amount into an electrical signal;

Step 7: Utilize the adjustment conversion circuit to amplify and filter the electrical signal. After the filter sensor completes the acquisition task, it is a very important link because the initial information collected by the sensor contains a lot of noise, and the amount of useful information is covered up, so filtering is necessary, so it is essential to use the adjustment conversion circuit for filtering;

Step 8: If the collection time arrives, then enter the interrupt program; otherwise, send the collected receiver;

Step 9: If the next collection round is entered, go back to step 5. Otherwise, wait for the shutdown command to shut down the entire sensor system.

#### 4. Result Analysis and Discussions.

**4.1. Sensor Materials and Assembly.** According to the theoretical design of the automatic measurement sensor, relevant materials are used to prepare a miniature pressure sensor. The dimensions of the sensor preparation materials are shown in Table 4.1.

The table's materials are assembled to prepare a finished automated measurement sensor. Due to the different content of subsequent tests, six finished samples were prepared with six copies of the same material. The expected standards of the finished automated measurement sensor prepared are as follows:

Accuracy:  $\leq \%F \cdot S \pm 0.10$ ;

Nonlinear:  $\leq \%F \cdot S \pm 0.13$ ;

Hysteresis:  $\leq \%F \cdot S \pm 0.12$ ;

Repeatability:  $\leq \%F \cdot S \pm 0.11$ .

The functional diagram of the pressure measurement system is shown in Figure 4.1. The system mainly comprises a capacitive micro-sensor, signal processing circuit, low-pass filter, amplification circuit, A/D conversion circuit, single-chip microcomputer and its peripheral devices. Capacitive micro-sensor converts the measured pressure change into capacitance change. The signal processing circuit synchronously detects the capacitance change signal and obtains a DC signal after filtering by a low-pass filter. We must amplify the signal to ensure direct analog-to-digital conversion of the signal and improve the signal's anti-interference ability and the instrument's sensitivity. The amplified DC voltage signal is transmitted to the single-chip microcomputer system through A/D conversion and then processed and analyzed by the computer.

**4.2. Sensor Performance Test .** The performance detection of an automatic measurement sensor is analyzed with the help of the following test items.

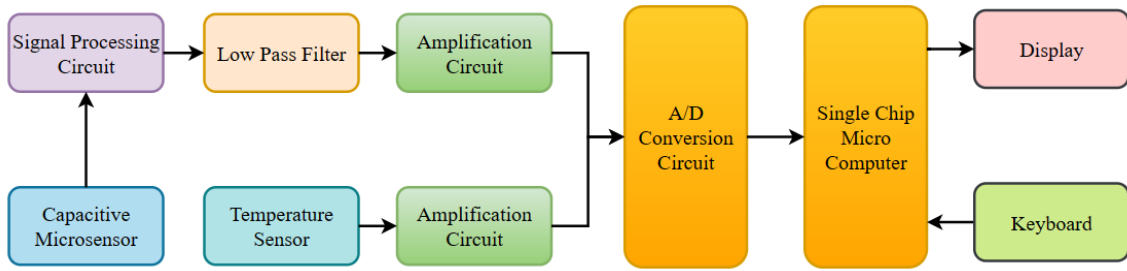


Fig. 4.1: Functional diagram of the pressure measurement system

1) *Accuracy test.* Accuracy is the error between the value collected by the sensor and the pressure value acting on the sensor. The test device is a universal pressure testing machine, and the designed sensor is placed directly under the lower plate of the testing machine. Then different pressure application values (5MPa to 50MPa) are set, the test is ten times, the absolute average value, and finally, the difference with the actual pressure value, and the verification difference is  $\leq \%F \cdot S \pm 0.10$ .

2) *Reliability.* Sensor reliability detection refers to the degree of sealing of the detection interface, whether air or electric leakage exists. The test devices for the above two phenomena are pressure leak detectors and megohmmeters. The former qualification standard is the average value  $\leq 0.05\%$  of the applied stable pressure value, and it is considered that there is no leakage problem at the interface. The latter qualification standard is the insulation resistance value  $\geq 50$  megohms, and it is considered that there is no leakage problem at the interface.

3) *Sensitivity.* Sensitivity refers to the degree to which the sensor's output changes as the input changes. The data required for the test comes from the data measured by the device. The sensitivity is calculated using Equation 4.1:

$$S = \frac{\partial C}{\partial P} = \frac{C_0}{2P} \left( \frac{1}{1 + \frac{Pd}{P_m g}} - \frac{\tanh^{-1} \sqrt{\frac{Pd}{P_m g}}}{\sqrt{\frac{Pd}{P_m g}}} \right) \times 100\% \quad (4.1)$$

In Equation 4.1, C represents the increment of the sensor output; g represents the distance between the initial voltage value of the sensor and the electrode;  $C_0$  represents the initial voltage value of the sensor;  $P_m$  represents the maximum pressure when the maximum deflection of the center of the diaphragm is equal to the constant d, and P represents the pressure of the outside gas.

4) *Nonlinearity.* Nonlinearity means that according to the time series, the fitted deviation between the curve drawn by the output of the measured value by the automated measurement sensor and the actual pressure curve. The measurement formula is shown in Equation 4.3:

$$R_L = \frac{\Delta L_{max}}{F_{YS}} \times 100\% \quad (4.2)$$

In the Equation,  $\Delta L_{max}$  represents the maximum deviation between the curve drawn by the measured value output by the automatic measurement sensor and the actual pressure curve;  $F_{YS}$  represents the full-scale output voltage value.

5) *Hysteresis.* Hysteresis refers to the maximum difference between the output voltage values of the two when the input value increases and decreases at the same test point within the full-scale range. The data sources required for the test are the same as above. The hysteresis can be calculated by Equation 4.4:

$$Y_H = \frac{\Delta C_{max}}{F_{YS}} \times 100\% \quad (4.3)$$

where  $\Delta C_{max}$  represents the maximum hysteresis error of the pressure sensor within the test range.  $F_{YS}$  represents the full-scale output voltage value.

Table 4.2: Performance evaluation of an automatic measurement sensor

Test items		Test results	Eligibility criteria
Precision		0.0451%	Qualified
Reliability	Pressure average	0.00363%	Qualified
	Insulation resistance value	68.44 megohms	Qualified
Sensitivity		0.0581%	Qualified
Nonlinearity		0.0740%	Qualified
Hysteresis		0.0264%	Qualified
Repeatability		0.0624%	Qualified

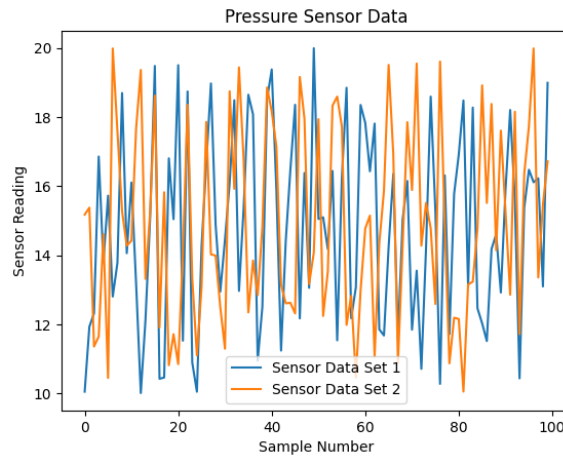


Fig. 4.2: Performance comparison of two different sensor data

6) *Repeatability*. The degree of agreement between the results of multiple consecutive measurements under the same test conditions required for the test is the same. The formula for finding the repeatability is given by Equation 4.5:

$$F = \frac{2a \sim 3a}{Y_{FS}} \times 100\% \quad (4.4)$$

where  $a$  represents the Bessel standard deviation.

The test results of the miniature pressure automatic measurement sensor designed by the author are shown in Table 4.2.

Table 4.2 compares the test qualification standards. The actual test results are within the range specified by the qualification standards, proving that the designed sensor meets expectations and can be used in actual pressure testing. Figure 4.2 serves as a visual aid for scrutinizing the performance of a pressure sensor over time, enabling a direct comparison between two distinct sets of sensor data.

Figure 4.3 shows that under the experimental conditions of different pressure application values (5MPa to 50MPa), the sensor's response time increases with pressure.

**5. Conclusion.** The sensor designed in this article showcases a broad spectrum of applications, highlighting its versatility in measuring and detecting various parameters. This adaptability significantly simplifies the data collection processes, catering to the needs of both individuals and professionals. However, among the ongoing exploration of sensor technology, a noticeable trend towards increased miniaturization becomes apparent, propelled by the pursuit of heightened precision in measurements. The author emphasizes the intricate design of sensitive elements, conversion components, and various circuits essential to the sensor's functionality.

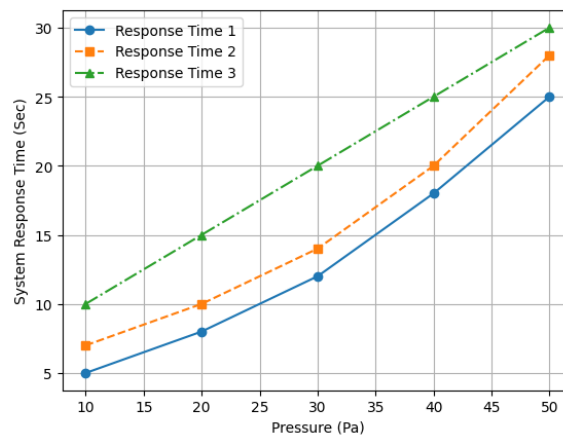


Fig. 4.3: System response time under different pressure values

Following the design phase, a meticulous performance testing protocol is implemented for the sensor products, ensuring compliance with rigorous product qualification standards. This comprehensive approach guarantees that the designed sensor meets and exceeds the required benchmarks, reinforcing reliability and efficiency across diverse applications.

#### REFERENCES

- [1] Kurmendra, & Kumar, R. . (2021). A review on rf micro-electro-mechanical-systems (mems) switch for radio frequency applications. *Microsystem Technologies*, 27(7), 2525-2542.
- [2] Boniface, M. , Plodinec, M. , Schlgl, R. , & Lunkenbein, T. . (2020). Quo vadis micro-electro-mechanical systems for the study of heterogeneous catalysts inside the electron microscope?. *Topics in Catalysis*, 63(15-18), 1623-1643.
- [3] Jena, S. , & Gupta, A. . (2021). Review on pressure sensors: a perspective from mechanical to micro-electro-mechanical systems. *Sensor Review*, 41(3), 320-329.
- [4] Song, P., Ma, Z., Ma, J., Yang, L., Wei, J., Zhao, Y., ... & Wang, X. (2020). Recent progress of miniature MEMS pressure sensors. *Micromachines*, 11(1), 56.
- [5] Lysenko, I. E. , Tkachenko, A. V. , Ezhova, O. A. , Konoplev, B. G. , & Sherova, E. V. . (2020). The mechanical effects influencing on the design of rf mems switches. *Electronics*, 9(2), 207.
- [6] Schmitt, P. , & Hoffmann, M. . (2020). Engineering a compliant mechanical amplifier for mems sensor applications. *Journal of Microelectromechanical Systems*, PP(99), 1-14.
- [7] Granados-Ortiz, F. J. , & Ortega-Casanova, J. . (2020). Mechanical characterization and analysis of a passive micro heat exchanger. *Micromachines*, 11(7), 668.
- [8] Liu, S. , Wang, K. , Wang, B. , Li, J. , & Zhang, C. . (2021). Size effect on thermo-mechanical instability of micro/nano scale organic solar cells. *Meccanica*, 57(1), 87-107.
- [9] Lin, H. , Y Li, Lam, J. , & Wu, Z. G. . (2021). Multi-sensor optimal linear estimation with unobservable measurement losses. *IEEE Transactions on Automatic Control*, PP(99), 1-1.
- [10] Evtikhiev, Kozlov, A. V. ,Krasnov, Rodin, V. G. , Starikov, R. S. , & Cheremkhin, P. A. . (2021). Estimation of the efficiency of digital camera photosensor noise measurement through the automatic segmentation of non-uniform target methods and the standard emva 1288. *Measurement Techniques*, 64(4), 296-304.
- [11] Zheng, T. , Yu, Z. , Wang, J. , & Lu, G. . (2020). A new automatic foot arch index measurement method based on a flexible membrane pressure sensor. *Sensors*, 20(10), 2892.
- [12] Dufour, D. , Noc, L. L. , Tremblay, B. , Tremblay, M. N. , & Topart, P. . (2021). A bi-spectral microbolometer sensor for wildfire measurement. *Sensors*, 21(11), 3690.
- [13] Zhang, F. , Li, J. , Lu, J. , & Xu, C. . (2021). Optimization of circular waveguide microwave sensor for gas-solid two-phase flow parameters measurement. *IEEE Sensors Journal*, PP(99), 1-1.
- [14] Offenzeller, C. , Knoll, M. , Voglhuber-Brunnmaier, T. , Hilber, W. , & Jakoby, B. . (2020). Screen printed sensor design for thermal flow velocity measurement with intrinsic compensation of thermal fluid conductivity. *IEEE Sensors Journal*, PP(99), 1-1.
- [15] Guan, X. , Zou, Y. , Shang, J. , Bian, X. , & Li, Q. . (2021). A mutual inductance sensor for cryogenic radial displacement measurement. *Cryogenics*, 115(5), 103263.
- [16] Feng, Y. , Tao, W. , Feng, Y. , Yin, X. , & Zhao, H. . (2020). High-precision width measurement method of laser profile

- sensor. *Sensor Review*, 40(6), 699-707.
- [17] Kim, S. G., Priya, S., & Kanno, I. (2012). Piezoelectric MEMS for energy harvesting. *MRS bulletin*, 37(11), 1039-1050.
- [18] Lyu, C. , Li, P. , Wang, D. , Yang, S. , & Sui, C. . (2020). High-speed optical 3d measurement sensor for industrial application. *IEEE Sensors Journal*, PP(99), 1-1.
- [19] Rayguru, M. M. , Elara, M. R. , Balakrishnan, R. , Muthugala, M. , & Samarakoon, S. . (2020). A path tracking strategy for car like robots with sensor unpredictability and measurement errors. *Sensors*, 20(11), 3077.
- [20] Zhao, L. , Zhang, Y. , Chen, Y. , Chen, Y. , Yi, G. , & Wang, J. . (2020). A fiber strain sensor with high resolution and large measurement scale. *IEEE Sensors Journal*, 20(6), 2991-2996.
- [21] Keshari, A. K. , Rao, J. P. , Murthy, A. , & Jayaraman. (2020). Design and development of instrumentation for the measurement of sensor array responses. *Review of Scientific Instruments*, 91(2), 024101.
- [22] Kamp, J. N. , Srensen, L. L. , Hansen, M. J. , Nyord, T. , & Feilberg, A. . (2021). Low-cost fluorescence sensor for ammonia measurement in livestock houses. *Sensors*, 21(5), 1701.
- [23] Kim, S. , & Lee, K. . (2020). Development of underground wireless saw integrated sensor measurement system using magnetic field. *Transactions of the Korean Institute of Electrical Engineers*, 69(6), 903-913.
- [24] Cecchi, S. , Spinsante, S. , Terenzi, A. , & Orcioni, S. . (2020). A smart sensor-based measurement system for advanced bee hive monitoring. *Sensors*, 20(9), 2726.
- [25] Li, C. , Li, B. , Huang, J. , & Li, C. . (2020). Developing an online measurement device based on resistance sensor for measurement of single grain moisture content in drying process. *Sensors*, 20(15), 4102.

*Edited by:* Venkatesan C

*Special issue on:* Next Generation Pervasive Reconfigurable Computing for High Performance Real Time Applications

*Received:* Sep 27, 2023

*Accepted:* Jan 22, 2024